Mechanism of linear and nonlinear optical effects of chalcopyrite $AgGaX_2$ (X=S, Se, and Te) crystals

Lei Bai, Zheshuai Lin, Zhizhong Wang, and Chuangtian Chen
Beijing Center For Crystal Research & Development, Technical Institute of Physics and Chemistry, Chinese Academy of Sciences, P.O. Box 2711, Beijing, 100080, China

Ming-Hsien Lee
Department of Physics, Tamkang University, Tamsui, Taipei 251, Taiwan

(Received 6 November 2003; accepted 27 January 2004)

The electronic band structures for $AgGaX_2$ (X=S, Se, Te) chalcopyrites have been calculated using a pseudopotential total energy method. First-principles calculations of the linear and nonlinear optical properties are presented for these crystals, with the electronic band structures obtained from pseudopotential method as input. The theoretical refractive indices and nonlinear optical coefficients are in good agreement with available experimental values. The origin of the nonlinear optical effects is explained through real-space atom-cutting analysis. The contribution of the GaX_2 group (X=S, Se, Te) for second harmonic generation (SHG) effect is dominant while that of the cation Ag is negligible. In addition, the percentage contribution to the SHG coefficients from the different bonds increase with increase of the bond order. © *2004 American Institute of Physics.*
[DOI: 10.1063/1.1687338]

I. INTRODUCTION

Nonlinear optical (NLO) crystals can significantly enhance laser performance by enabling wavelength shifting and tuning over a broad spectral range. Among these, infrared (IR) and even far-IR crystals can extend the near-IR laser wavelengths (for example 1.064 μm) into the mid-IR spectral range through frequency-down conversion such as optical parametric oscillation and amplification, and can also convert far-IR wavelengths (for example, 10.6 μm of the CO_2 laser) to the mid-IR spectral range (from 5 μm to near 2.0 μm) through frequency conversion. Most of the IR NLO crystals that have been used in the frequency conversion processes belong to the chalcopyrite structure, for example, $AgGaX_2$ (M=S, Se, and Te) and $ZnGeX_2$ (X=P and As) families, because they have very large d_{ij} coefficients (about 50–100 pm/V), a wide transparancy range (0.5–17 μm), as well as moderate birefringence (0.05–0.09). A recent review of the emergence of chalcopyrites as nonlinear optical materials was published by Ohmer and Pandey,[1] who listed the properties of various infrared nonlinear semiconductors. Some of these are cited here in Table I. As $\chi^{(2)}$ increases rapidly with decreasing band gap, the coefficient for $AgGaTe_2$ should be significantly larger than the $\chi^{(2)}$ of the IR NLO crystal $AgGaSe_2$. Up to now no experimental value for $\chi^{(2)}$ of $AgGaTe_2$ has been reported. Jackson *et al.*[2] have estimated it by two methods obtaining the values of 170 and 220 pm/V, respectively. The traditional Miller's rule[3] predicts a value of 344 pm/V for $AgGaTe_2$.

However, although these crystals have been widely used for mid- and far-IR laser frequency conversion only a few have been examined theoretically. For example, Rashkeev and colleagues[4] have systematically studied the electronic structure and optical properties of a class of ternary compounds with formula ABC_2 (A=Zn, Cd; B=Si, Ge; C=As, P) that crystallize in the chalcopyrite structure, and have discussed the intraband and interband contributions. Recently, the electronic band structures for a number of chalcopyrie crystals in both II–IV–V_2 (II=Cd, Zn, IV=Si, Ge, and V=P, As) and I–III–VI_2 (I=Ag, III=Ga, In and VI=S, Se, Te) families using the linear muffin-tin orbital method have been calculated[5] however, only the trends in $\chi^{(2)}$ coefficients have been discussed.

In recent years, we have reviewed the calculation of the second-harmonic generation (SHG) coefficients based on first principles and suggested an improved calculation formula.[6,7] The method requires an input describing the electronic band structure, which we obtained from CASTEP,[8] a plane-wave pseudopotential total energy package. We have used our method to successfully calculate the linear and nonlinear optical responses of a series of important NLO crystals such as BBO,[6] the LBO family,[9] BIBO,[10] KBBF,[11] $SrBeO_4$,[12] KDP and urea.[13] In addition, the origins of the SHG effects of these crystals were clearly explained by using a real-space atom-cutting method. This analysis method isolates the contribution of individual or groups of atoms by removing spatial localized wave functions from the evaluation.

The goal of this work is to calculate the electronic structure, and linear and nonlinear optical parameters of $AgGaX_2$ (X=S, Se, and Te) from first principles quantum mechanics and to give an explanation of the origin of the optical responses.

II. METHOD AND COMPUTATIONAL DETAILS

The plane-wave pseudopotential total energy software package CASTEP is used for solving the electronic and band structures. The results are then applied to the calculation of the optical responses. The theoretical basis of CASTEP is the

TABLE I. A partial list of infrared nonlinear semiconductors and their properties (Ref. 1).

Compound	Second NLO coefficients pm/V	Transparency range microns	Absorption coefficient cm^{-1}	Thermal conductivity W/m K	Band gap eV
GaAs	90	1.1–17	0.005	52	1.42
$AgGaS_2$	11	0.48–11.4	0.04	1.5	2.73
$AgGaSe_2$	33	0.76–17	0.002	1.1	1.833
$AgGaTe_2$	51[a]	0.91–23	b	0.8	1.36
$ZnGeP_2$	75	0.74–12	0.4	36	2.0
$CdGeAs_2$	217	2.7–18	0.46	6.7	0.57

[a]Conservative estimate.
[b]To be determined.

density functional theory (DFT) with the local-density approximation (LDA).[14] Within such a framework the preconditioned conjugated gradient (CG) band-by-band method[15] used in CASTEP ensures a robust and efficient search of the energy minimum of the electronic structure ground state. The optimized pseudopotentials[16–18] in the Kleinman–Bylander form for Ag, Ga, S, Se, and Te allow us to use a small plane-wave basis set without compromising the accuracy required by our study. For the plane wave basis set the energy cutoffs of 300, 500, and 800 eV were used for $AgGaS_2$, $AgGaSe_2$, and $AgGaTe_2$, respectively.

It is well known that the band gap calculated by the local density approach is usually smaller than the experimental data due to the discontinuity of exchange–correlation energy. A scissors operator[19,20] is hence used to shift upward all the conduction bands in order to agree with measured values of the band gap.

The static limit of the SHG coefficients plays the most important role in the application of SHG crystals. Our group and collaborators have reviewed various methods for calculating the SHG coefficients,[6,13] and finally adopted the formula of Rashkeev *et al.*[21] after some modification,

$$\chi^{\alpha\beta\gamma}=\chi^{\alpha\beta\gamma}(\mathrm{VE})+\chi^{\alpha\beta\gamma}(\mathrm{VH})+\chi^{\alpha\beta\gamma}(\text{two bands}).$$

Here $\chi^{\alpha\beta\gamma}(\mathrm{VE})$ and $\chi^{\alpha\beta\gamma}(\mathrm{VH})$ are the contributions to $\chi_i^{(2)}$ from the virtual-electron and virtual-hole processes, respectively; $\chi^{\alpha\beta\gamma}(\text{two bands})$ is the contribution to $\chi_i^{(2)}$ from the two-band processes. The formulas for calculating $\chi^{\alpha\beta\gamma}(\mathrm{VE})$, $\chi^{\alpha\beta\gamma}(\mathrm{VH})$, and $\chi^{\alpha\beta\gamma}(\text{two bands})$ are given in Ref. 6.

To investigate the influence of the ions on the crystal optical response, a real-space atom-cutting method has been used. With this method the contribution of ion A to the nth-order susceptibility denoted as $\chi^{(n)}(A)$ is obtained by cutting out all ions except A from the original wave functions $\chi^{(n)}\times(A)=\chi^{(n)}$ (all ions except A are cut).

All the $AgGaX_2$ (X=S, Se, and Te) crystals are reported to have the chalcopyrite structure with the $\bar{4}2m$ space group, as shown in Fig. 1. In our calculations we took the lattice parameters of $AgGaS_2$, $AgGaSe_2$, and $AgGaTe_2$ to be $a=b=5.757$ and $c=10.304$ Å,[22] $a=b=5.973$ and $c=10.85$ Å,[23] and $a=b=6.288$ and $c=11.949$ Å,[23–25] respectively.

III. RESULTS AND DISCUSSION

A. Energy bands

The energy bands of $AgGaS_2$, $AgGaSe_2$, and $AgGaTe_2$ crystals were calculated. The calculated bands of three crystals along the lines of high symmetry points in the Brilloiun zone are shown in Figs. 2(a), 2(b), and 2(c), respectively. It is obvious that the shapes of the bands in Figs. 2(a), 2(b), and 2(c) are very similar due to the similarity of the structures of the three crystals. Both the top of the valence band (VB) and the bottom of the conduction band (CB) are at the gamma point (G). The direct band gaps of 2.23, 1.42, and 0.75 eV are obtained and listed in Table II, all being smaller than the corresponding experimental values of 2.63, 1.743, and 1.316 eV, respectively. It is well known that the calculated band gaps from the density functional theory are usually smaller than the corresponding experimental values. A semiempirical

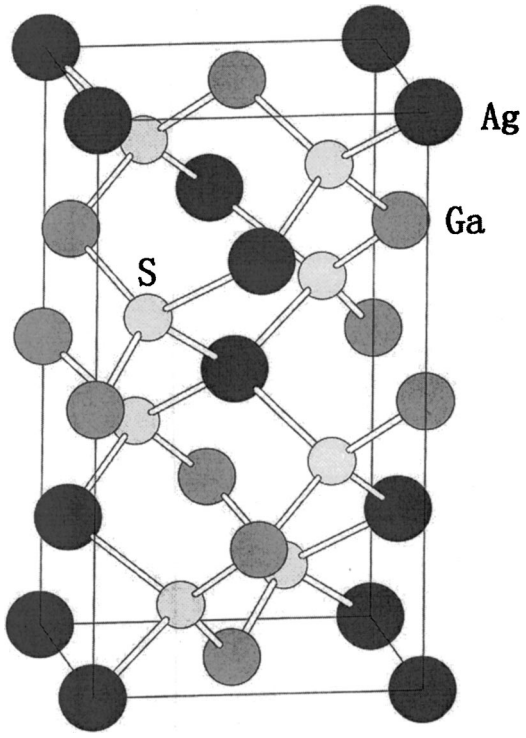

FIG. 1. Unit cell of the $AgGaS_2$ crystal.

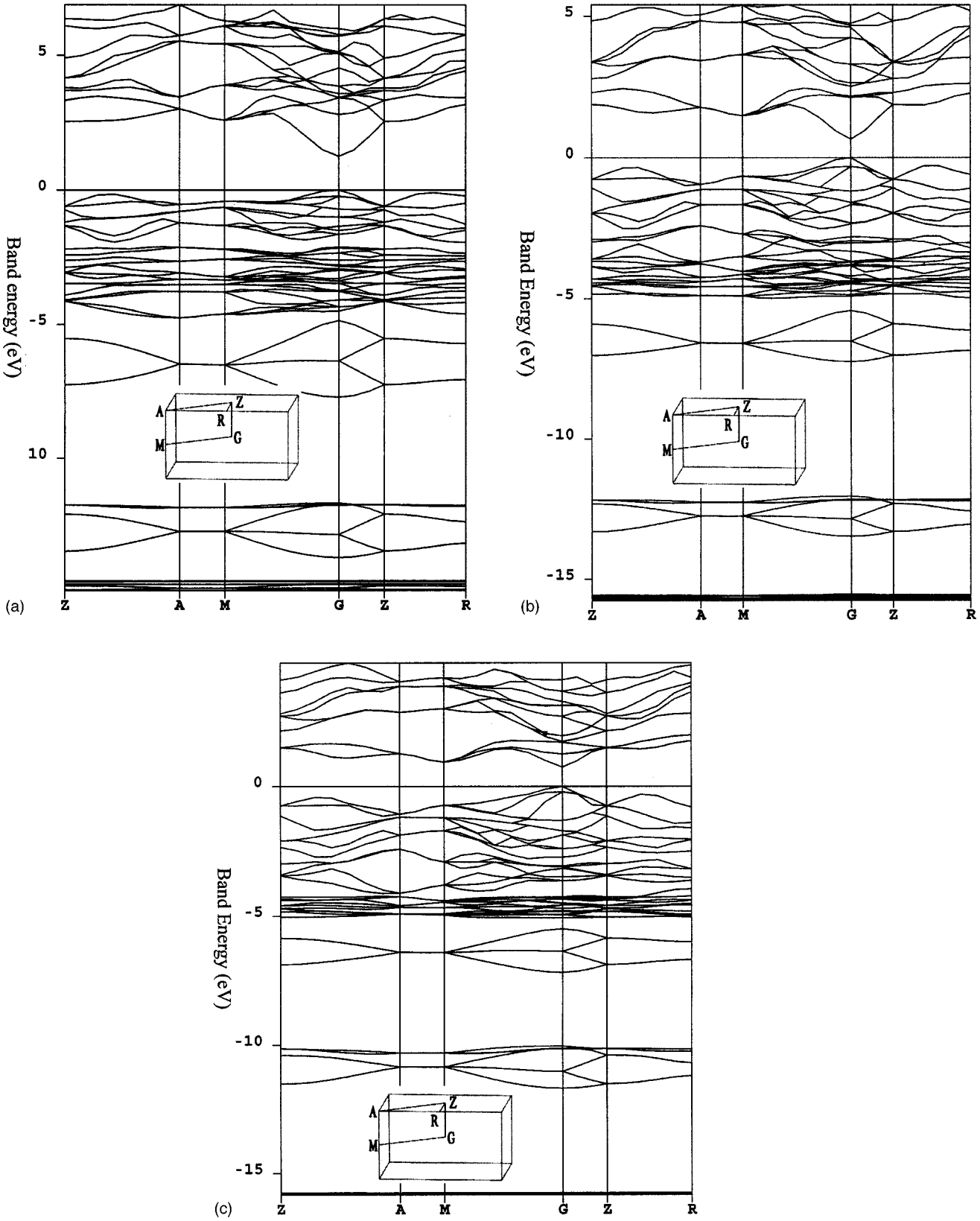

FIG. 2. Band structure of $AgGaS_2$, $AgGaSe_2$, and $AgGaTe_2$: (a) $AgGaS_2$, (b) $AgGaSe_2$, and (c) $AgGaTe_2$.

correction for this is necessary to obtain meaningful results. To fit the measured absorption edge, the energy scissors operator is commonly employed to shift all conduction bands[24,25] upwards before calculating the response expressions. For the calculations of $AgGaS_2$, $AgGaSe_2$, and $AgGaTe_2$ a scissors energy of 0.40, 0.50, and 0.56 eV was used, respectively. Figures 3(a), 3(b), and 3(c) show the partial density of state (PDOS) projected on the constitutional

TABLE II. Calculated and experimental values of linear and nonlinear optical coefficients for $AgGaX_2$ (X=S, Se, and Te).[a]

	$AgGaS_2$	$AgGaSe_2$	$AgGaTe_2$
Energy gap (eV)	2.23	1.42	0.75
Energy scissors	0.40	0.50	0.56
n_0	2.5840(2.4486)	2.9798(2.8932)	3.2678(2.9859)
n_e	2.5530(2.3954)	2.9358(2.8452)	3.2799(3.0047)
$\Delta n=n_0-n_e$	0.0310(0.0532)	0.0440(0.0480)	−0.0115(−0.0188)
d_{36} (pm/V)	14.10(11.0,12.5)	45.20(33.0)	99.5

[a]Values in parentheses are experimental ones from V. G. Dimitriev *et al.*, *Handbook of Nonlinear Optical Crystals*, 2nd revised ed. (Springer, Berlin, 1977).

atoms of $AgGaS_2$, $AgGaSe_2$, and $AgGaTe_2$ crystals, respectively. Obviously, for $AgGaS_2$ the orbitals of silver and sulfur atoms (or selenium or tellurium for $AgGaSe_2$ and $AgGaTe_2$) contribute more in both valence and conduction bands than the gallium atom. For the three crystals considered the peaks of both silver and gallium are slightly shifted. The widths of the valence bands of $AgGaS_2$, $AgGaSe_2$, and $AgGaTe_2$ decrease gradually from wide (15 eV) to narrow (12 eV). In fact, this is the origin of the decreasing band gaps for the three crystals considered.

B. Linear optical response

It is known that the refractive indices can be obtained theoretically from the dielectric function. The imaginary part of the dielectric function can be calculated with the matrix elements which describe the electronic transitions between the ground state and the excited states in the crystal considered. In Table II we list the theoretical refractive indices and birefringence of three crystals. The calculated refractive indices are in reasonably good agreement with experimental values. The calculated birefringences are in accordance with the fact that both $AgGaS_2$, $AgGaSe_2$ crystals are negative uniaxial crystals. In addition, $AgGaTe_2$ is positive birefringent.

To investigate the respective contributions of different ionic groups, we employ the real-space atom-cutting method.[11] With this method the contribution of ion A to the nth-order susceptibility, denoted as $\chi^{(n)}(A)$, is obtained by cutting all ions except A from the original wave functions, i.e., $\chi^{(n)}(A)=\chi^{(n)}_{\text{All ions except } a \text{ are cut}}$. In a previous paper we found that the charge density around the cation is spherical.[6] The same situation is met by these crystals, Figs. 4(a) and 4(b) show the charge density contour maps of the $AgGaS_2$ crystal. Apparently, the charge density around Ag is also spherical. Thus we first choose the cutting radius of Ag as 1.30 Å. Following the rule of keeping the cutting spheres of the cation and S (or Se, Te) in contact and not overlapping, we choose the cutting radii of Ga and S (or Se, Te) atoms to be 0.90 and 1.45 Å (or 1.57, 1.80 Å), respectively. The cutting radii used in calculations are about average of atomic covalent and ionic radii. The atom-cutting analysis results are listed in Table III. It is obvious that even the orbitals of the silver atom contribute more in both valence and conduction bands than that of the gallium atom but the orbitals of the silver atom only contribute to the absolute values of refractive indices but almost not to birefringence because of the spherical charge density around the Ag atom. On the other hand, the contribution of the GaS_2 (or $GaSe_2$, $GaTe_2$) group to both of the absolute values and birefringence are still dominant because the bonds of Ga–S (or Ga–Se, Ga–Te) have more covalent part than those of Ag–S (or Ag–Se, Ag–Te).

C. Nonlinear optical response

It is well known that the second order susceptibility $\chi^{(2)}$ is twice of the SHG coefficient d_{ij}. For the above-mentioned chalcopyrite crystals with $\bar{4}2m$ space group symmetry the only independent SHG coefficient is $d_{14}=d_{36}$. The theoretical nonlinear coefficients of $AgGaS_2$, $AgGaSe_2$, and $AgGaTe_2$ are 14.10, 45.20, and 99.50 pm/V, respectively, and are listed in Table II. The theoretical SHG coefficients d_{36} or $\chi^{(2)}_{xyz}$ are in good agreement with the available experimental data for $AgGaS_2$ and $AgGaSe_2$. Our calculations give a prediction for $AgGaTe_2$ which is quantitatively in accordance with empirical predictions.[2,3] These calculations clearly reveal the effects of chemical substitutions within the $AgGaS_2$ family. In this case, we see a systematic increase of $\chi^{(2)}$ with decreasing gap and with the progression from S to Se to Te as anion. The extremely large value of the SHG coefficient in $AgGaTe_2$ is due to the fact that it has the smallest band gap in the three crystals considered.

Results of the atom-cutting method applied to the calculation of SHG coefficients are also given in Table III. In the calculations we used the same cutting radii as in the cutting analysis calculation of the linear response. Obviously, the contributions to the SHG coefficients of the GaS_2 (or $GaSe_2$ or $GaTe_2$) group are dominant, and the contribution of cation Ag is about 2% for the three crystals. On the other hand, we have also discussed the contributions from different chemical bonds by the cutting analysis method. The results are listed in Table IV. For $AgGaS_2$, $AgGaSe_2$, and $AgGaTe_2$, the percentages of the contribution to SHG coefficients from GaS, GaSe, and GaTe bonds are 73, 70, and 60, respectively, and from AgS, AgSe, and AgTe bonds they are 20%, 22%, and 36%, respectively. Obviously, the percentage of contributions from the different bonds increase with increase of the bond order. This is due to the fact that for a chemical bond the larger the bond order, the bigger the covalency. The contribution from the AgGa bond is about 5%. This is due to the

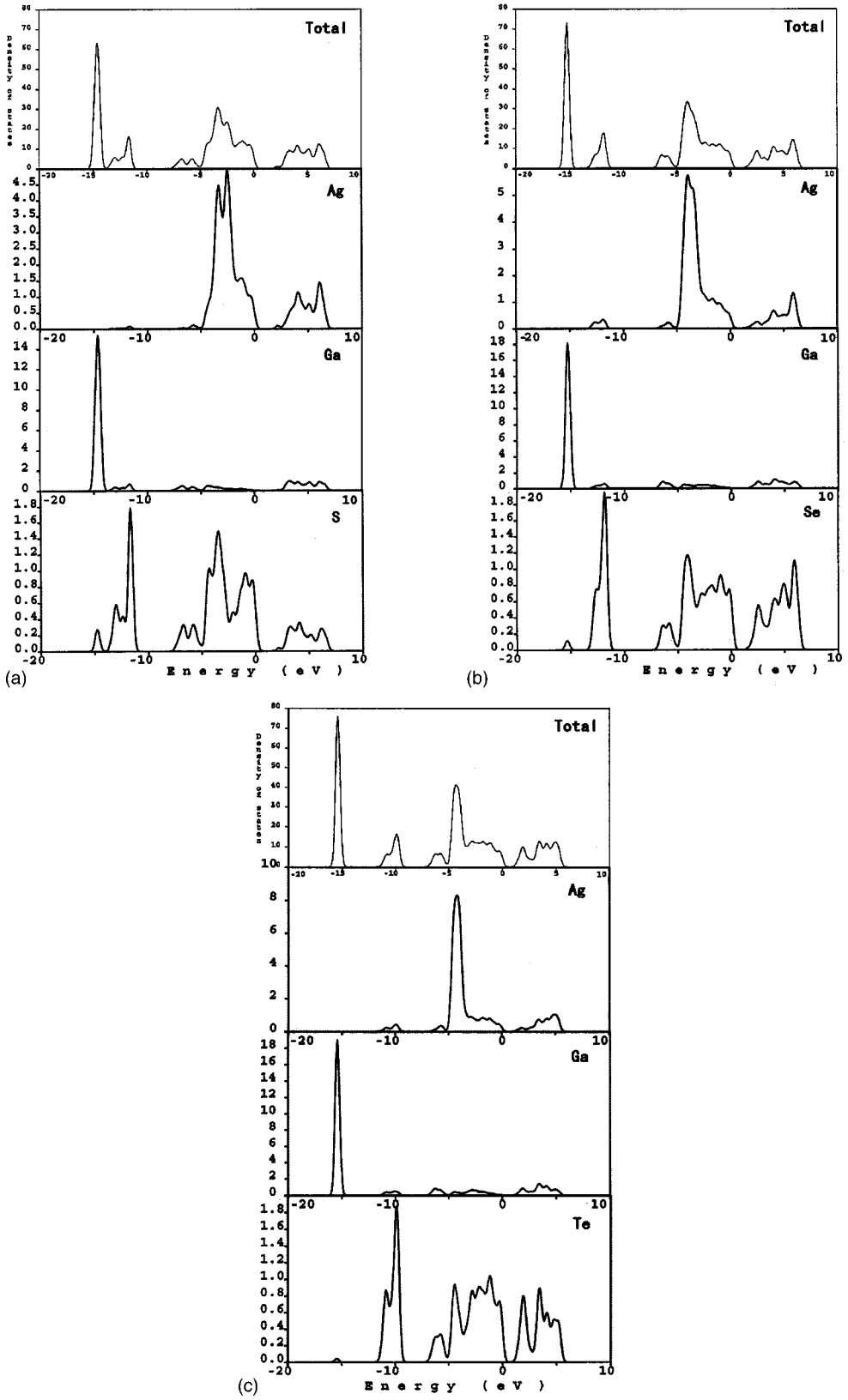

FIG. 3. DOS and PDOS plots of $AgGaS_2$, $AgGaSe_2$, and $AgGaTe_2$.

small overlap of the electron clouds of the Ag and Ga atoms. In the cutting analysis for chemical bonds, the sum of the partial NLO coefficients from all the bonds in each crystal is larger than that of the complete crystal because some of the atoms have been repeatedly used.

IV. CONCLUSION

The electronic band structures of three Ag–Ga–chalcogenides have been calculated by first-principles theory, and the linear and nonlinear optical responses also computed

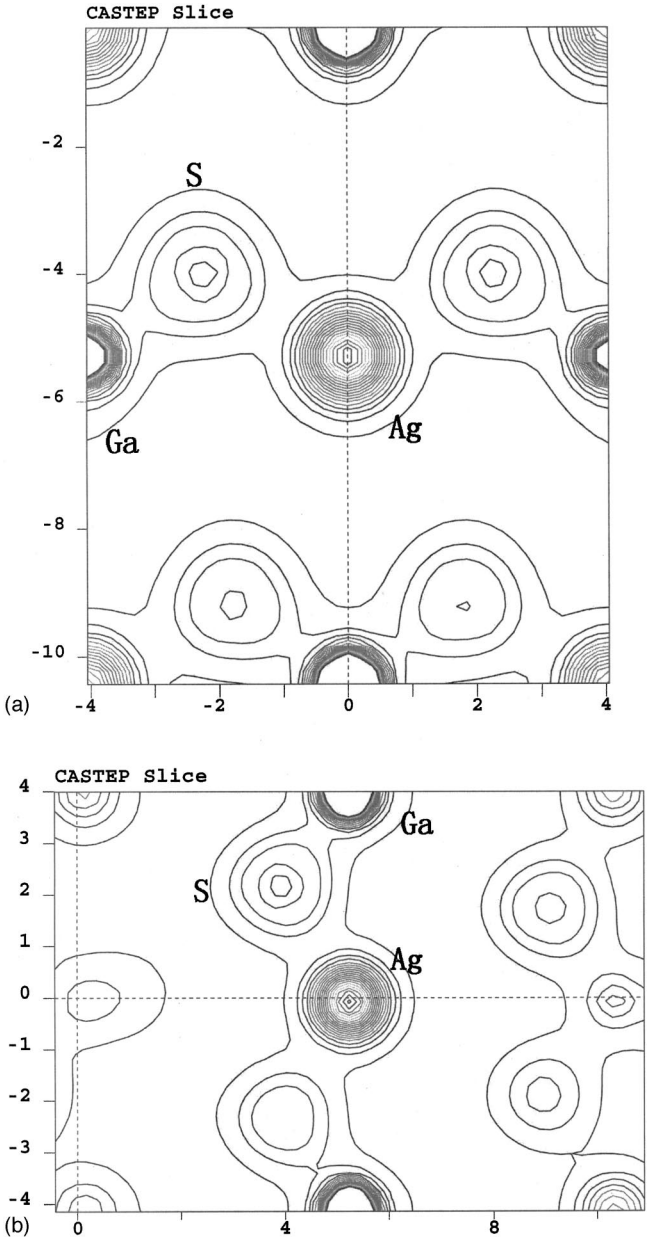

FIG. 4. Charge density contour map of $AgGaS_2$: (a) in plane of two Ag–S bonds, (b) on plane of the Ag, Ga, and S atoms.

TABLE III. Calculated vales of linear and nonlinear optical coefficients and cutting analysis for $AgGaX_2$ (X=S, Se, and Te).

Crystal		Contribution			
$AgGaS_2$		Ag	GaS_2	Sum	Origin
	n_0	1.4373	2.3503		2.5840
	n_e	1.4341	2.3364		2.5530
	Δn	0.0032	0.0139	0.0171	0.0310
	d_{36} (pm/V)	0.52	14.84	15.36	14.1
$AgGaSe_2$		Ag	$GaSe_2$		Origin
	n_0	1.4676	2.7355		2.9798
	n_e	1.4630	2.7275		2.9358
	Δn	0.0040	0.0080	0.0120	0.0440
	d_{36} (pm/V)	1.18	46.25	47.43	45.20
$AgGaTe_2$		Ag	$GaTe_2$		Origin
	n_0	1.4442	3.0090		3.2684
	n_e	1.4497	3.0541		3.2799
	Δn	−0.0055	−0.0451	−0.0506	−0.0115
	d_{36} (pm/V)	2.22	90.0	92.2	99.5

TABLE IV. Calculated bond orders and contributions to d_{36} from different bonds.

	Ga–X		Ag–X		Ag–Ga		
	Bond ord.	d(GaX)	Bond ord.	d(AgX)	Bond ord.	d(AgGa)	Sum
$AgGaS_2$	0.55	14.84	0.25	4.17		1.34	20.31
		73%		20%		6%	100%
$AgGaSe_2$	0.52	46.25	0.27	15.0		4.43	65.68
		70%		23%		6.7%	100%
$AgGaTe_2$	0.34	90.0	0.40	52.5		7.6	150.1
		60%		35%		5%	100%

based on their band wave functions and energies. The theoretical values of the refractive indices and SHG coefficients d_{36} or $\chi^{(2)}_{123}$ are in good agreement with the available experimental data for $AgGaS_2$ and $AgGaSe_2$. The results clearly reveal the trend of increasing $\chi^{(2)}_{123}$ from S to Se to Te. The smaller the energy gap, the larger the value of $\chi^{(2)}$.

The results of real-space atom-cutting analysis present an explanation of the origin of the linear and nonlinear optical responses. The dominant contributions to the linear and nonlinear optical responses of three crystals considered are from the GaS_2 (or $GaSe_2$ or $GaTe_2$) group. On the other hand, the percentage of contribution to the SHG coefficients from the different bonds increase with increase of the bond order.

ACKNOWLEDGMENTS

This work was supported by the Chinese National Basic Research Project and National Science Foundation 90203016. Support in computing facilities from the Computer Network Information Center is gratefully acknowledged. L.Z.S. is grateful for the support from the K. C. Wang Education Foundation, Hong Kong, and M.H.L. for support from NSC 89-211-M-032-026.

[1] M. C. Ohmer and R. Pandey, MRS Bull. **23**, 16 (1998).
[2] A. G. Jackson, M. C. Ohmer, and S. R. Leclair, Infrared Phys. Technol. **38**, 233 (1997).
[3] R. C. Miller and W. A. Nordland, Phys. Rev. B **2**, 4896 (1970).
[4] S. N. Rashkeev, S. Limpijumnong, and W. R. L. Lambrecht, Phys. Rev. B **59**, 2737 (1999).
[5] W. R. L. Lambrecht, S. N. Rashkeev, S. Limpijumnong, and B. Segall, Symposium on Infrared Applications of Semiconductors III, 29 November–2 December 1999.
[6] J. Lin, M. H. Lee, Z. P. Liu, C. T. Chen, and C. J. Pickard, Phys. Rev. B **60**, 13380 (1999).
[7] Z. S. Lin, J. Lin, Z. Z. Wang *et al.*, J. Phys.: Condens. Matter **13**, R369 (2001).
[8] CASTEP 3.5 program developed by Molecular Simulation Inc., 9685 Scranton Road, San Diego, CA 92121 (1997).
[9] Z. S. Lin, Z. Z. Wang, C. T. Chen, and M. H. Lee, Phys. Rev. B **62**, 1757 (2000).
[10] Z. S. Lin, Z. Z. Wang, C. T. Chen, and M. H. Lee, J. Appl. Phys. **90**, 5585 (2001).
[11] Z. S. Lin, Z. Z. Wang, C. T. Chen, S. K. Chen, and M. H. Lee, Chem. Phys. Lett. **367**, 523 (2003).
[12] Z. S. Lin, Z. Z. Wang, C. T. Chen, H. T. Yang, and M. H. Lee, J. Chem. Phys. **117**, 2809 (2002).
[13] Z. S. Lin, Z. Z. Wang, C. T. Chen, and M. H. Lee, J. Chem. Phys. **118**, 2349 (2003).
[14] R. G. Parr and W. T. Yang, *Density Functional Theory of Atom-Molecules* (Oxford University Press, Oxford, 1989).

[15] M. C. Payne, M. P. Teter, D. C. Allan, T. A. Arias, and J. D. Joannopoulos, Rev. Mod. Phys. **64**, 1045 (1992).
[16] A. M. Rappe, K. M. Rabe, E. Kaxiras, and J. D. Joannopulos, Phys. Rev. B **41**, 1227 (1990).
[17] J. S. Lin, A. Qtseish, M. C. Payne, and V. Heine, Phys. Rev. B **47**, 4174 (1993).
[18] M.-H. Lee, J.-S. Lin, M. C. Payne, V. Heine, V. Milman, and S. Crampin (unpublished).
[19] R. W. Godby, M. Schluter, and L. J. Sham, Phys. Rev. B **37**, 10159 (1988).
[20] C. S. Wang and B. M. Klein, Phys. Rev. B **24**, 3417 (1981).
[21] S. N. Rashkeev, W. R. L. Lambrecht, and B. Segall, Phys. Rev. B **57**, 3905 (1998).
[22] S. C. Abrahams and J. L. Bernstein, J. Chem. Phys. **59**, 1625 (1973).
[23] H. Hahn, G. Frank, W. Klingler, and A. D. Meyer, Z. Anorg. Allg. Chem. **271**, 153 (1953).
[24] P. Kistaiah, Y. C. Venudar, K. Sathyanarayana Murthy, L. Iyengar, and K. V. Krishna, J. Appl. Crystallogr. **14**, 281 (1981).
[25] A. Burger, J.-O. Ndap *et al.*, J. Cryst. Growth **225**, 505 (2001).